Comparison of heat-inactivated and infectious SARS-CoV-2 across indoor surface materials shows comparable RT-qPCR viral signal intensity and persistence

Rodolfo A. Salido[1,2], Victor J. Cantú[1,2], Alex E. Clark[3], Sandra L. Leibel[4,5], Anahid Foroughishafiei[2], Anushka Saha[2], Abbas Hakim[6], Alhakam Nouri[6], Alma L. Lastrella[6], Anelizze Castro-Martínez[6], Ashley Plascencia[6], Bhavika Kapadia[6], Bing Xia[6], Christopher Ruiz[6], Clarisse A. Marotz[4,6], Daniel Maunder[6], Elijah S. Lawrence[6], Elizabeth W. Smoot[6], Emily Eisner[6], Evelyn S. Crescini[6], Laura Kohn[7], Lizbeth Franco Vargas[6], Marisol Chacón[6], Maryann Betty[4,6,8], Michal Machnicki[6], Min Yi Wu[6], Nathan A. Baer[6], Pedro Belda-Ferre[4,6], Peter De Hoff[5,6,9], Phoebe Seaver[6], R. Tyler Ostrander[6], Rebecca Tsai[4,6], Shashank Sathe[5,6,10], Stefan Aigner[5,6,10], Sydney C. Morgan[5,9], Toan T. Ngo[6], Tom Barber[6], Willi Cheung[5,6,11], Aaron F. Carlin[3], Gene W. Yeo[5,10], Louise C. Laurent[5,9], Rebecca Fielding-Miller[7,14], Rob Knight[2,4,12,13,14].

1. These authors contributed equally
2. Department of Bioengineering, University of California, San Diego, La Jolla, CA 92093, USA
3. Division of Infectious Diseases and Global Public Health, Department of Medicine; University of California San Diego School of Medicine, 9500 Gilman Drive, La Jolla, California 92093, USA
4. Department of Pediatrics, University of California San Diego, La Jolla, CA
5. Sanford Consortium of Regenerative Medicine, University of California San Diego, La Jolla, CA
6. Expedited COVID Identification Environment (EXCITE) Laboratory, Department of Pediatrics, University of California San Diego, La Jolla, CA
7. Herbert Wertheim School of Public Health, University of California, San Diego 9500 Gilman Drive, La Jolla, CA 92093
8. Rady Children's Hospital, San Diego, CA
9. Department of Obstetrics, Gynecology, and Reproductive Sciences, University of California San Diego, USA
10. Dept of Cellular and Molecular Medicine, University of California San Diego, La Jolla, CA
11. San Diego State University, San Diego, CA
12. Department of Computer Science and Engineering, University of California San Diego, La Jolla, CA, USA
13. Center for Microbiome Innovation, Jacobs School of Engineering, University of California San Diego, La Jolla, CA, USA
14. Co-corresponding authors

Abstract

Environmental monitoring in public spaces can be used to identify surfaces contaminated by persons with COVID-19 and inform appropriate infection mitigation responses. Research groups have reported detection of Severe Acute Respiratory Syndrome Coronavirus 2 (SARS-CoV-2) on surfaces days or weeks after the virus has been deposited, making it difficult to estimate when an infected individual may have shed virus onto a SARS-CoV-2 positive surface, which in turn complicates the process of establishing effective quarantine measures. In this study, we determined that reverse transcription-quantitative polymerase chain reaction (RT-qPCR) detection of viral RNA from heat-inactivated particles experiences minimal decay over seven

days of monitoring on eight out of nine surfaces tested. The properties of the studied surfaces result in RT-qPCR signatures that can be segregated into two material categories, rough and smooth, where smooth surfaces have a lower limit of detection. RT-qPCR signal intensity (average quantification cycle (*Cq*)) can be correlated to surface viral load using only one linear regression model per material category. The same experiment was performed with infectious viral particles on one surface from each category, with essentially identical results. The stability of RT-qPCR viral signal demonstrates the need to clean monitored surfaces after sampling to establish temporal resolution. Additionally, these findings can be used to minimize the number of materials and time points tested and allow for the use of heat-inactivated viral particles when optimizing environmental monitoring methods.

Importance

Environmental monitoring is an important tool for public health surveillance, particularly in settings with low rates of diagnostic testing. Time between sampling public environments, such as hospitals or schools, and notifying stakeholders of the results should be minimal, allowing decisions to be made towards containing outbreaks of coronavirus disease 2019 (COVID-19). The Safer At School Early Alert program (SASEA) [1], a large-scale environmental monitoring effort in elementary school and child care settings, has processed >13,000 surface samples for SARS-CoV-2, detecting viral signals from 574 samples. However, consecutive detection events necessitated the present study to establish appropriate response practices around persistent viral signals on classroom surfaces. Other research groups and clinical labs developing environmental monitoring methods may need to establish their own correlation between RT-qPCR results and viral load, but this work provides evidence justifying simplified experimental designs, like reduced testing materials and the use of heat-inactivated viral particles.

Intro

Development and characterization of methods for environmental monitoring of Severe Acute Respiratory Syndrome Coronavirus 2 (SARS-CoV-2) remain important areas of research for identifying and mitigating potential outbreaks as the global pandemic continues. Environmental monitoring offers indirect detection of possibly infectious individuals through noninvasive sampling. In spaces with relatively consistent occupants, detection of SARS-CoV-2 from environmental samples can help identify COVID-19-infected individuals, ideally before further transmission. Environmental monitoring can also alert public health leadership to the potential presence of an infection even in settings with low diagnostic testing uptake, allowing for the implementation of enhanced non-pharmaceutical interventions (i.e., double masking, increased hand hygiene, improved ventilation efforts) even in the absence of positive diagnostic tests.

SARS-CoV-2 particles are shed by symptomatic and asymptomatic carriers [**2**] and have been detected on various surfaces [**3, 4, 5, 6**]. Viral signatures have been demonstrated to persist up to 4 weeks in bulk floor dust collected from a room with a quarantined individual [6]. Previous environmental monitoring studies have detected SARS-CoV-2 on surfaces contaminated by infected individuals in hospitals and congregate care facilities [**7, 8, 9, 10, 11**]. Thus, indoor

surface sampling can be valuable for detection of infected persons indoors, where transmission risk is highest [**12**]. The Safer At School Early Alert program (SASEA) [**1**] uses environmental monitoring and collected over 13,000 surface swabs, but we need more information to clarify what these data are telling us over time.

We sought to characterize temporal dynamics underlying detection of SARS-CoV-2 signals from surface swabs from a variety of common indoor surface types using Reverse Transcription-quantitative Polymerase Chain Reaction (RT-qPCR). The Centers for Disease Control and Prevention (CDC) maintains that the risk of fomite transmission of SARS-CoV-2 is low [**13**]. Our study focuses not on transmission, but rather on whether and how negative and positive RT-qPCR detection from surface swabs can enable decision-making in outbreak mitigation, focused clinical testing of individuals, and safe reopening of high-traffic, public spaces.

We used RT-qPCR to detect heat-inactivated viral particles on nine surface materials, and monitored the persistence of the heat-inactivated virus for 7 days. Each material - acrylic, steel, glass, ceramic tile, melamine-finished particleboard (MFP), painted drywall, vinyl flooring, and two different carpets (olefin and polyester) - was divided into 5 cm by 5 cm grids, and each 25 cm^2 square surface of the grid was inoculated with 10 µL of either a dilution series of heat-inactivated SARS-CoV-2 particles or water. The 8-point dilution series was based on viral genomic equivalents (GEs) as measured by digital droplet PCR (ddPCR).The inoculum dried for 1 hr before swabbing. Every 24 hours post-inoculation an unswabbed section of each material grid was sampled, for a total of seven days including the initial post-inoculation swab.

To determine whether use of heat-inactivated viral particles in testing and validating environmental monitoring methods reflects results obtained using infectious virus, we compared detection of heat-inactivated SARS-CoV-2 (strain WA-1, SA-WA1/2020) and of authentic, infectious SARS-CoV-2 (variant of concern Beta, isolate B.1.351, hCoV-19/USA/MD-HP01542/2021) on two materials under biosafety level 3 (BSL-3) conditions.

Results

Linear regression of signal intensity (average *Cq* of viral gene calls) on elapsed time since inoculation (days) for each dilution showed minimal decay of viral RNA on 8 of 9 surface types over 6 days (Fig. 1). The average decay slope for each surface type (m-bar) did not differ significantly from zero (mean=0.0425, s.d.=0.207). RT-qPCR signal decayed with time only on glass (m-bar=0.396, s.d.=0.160, differing from the population mean by >1.5 standard deviations).

Figure 1

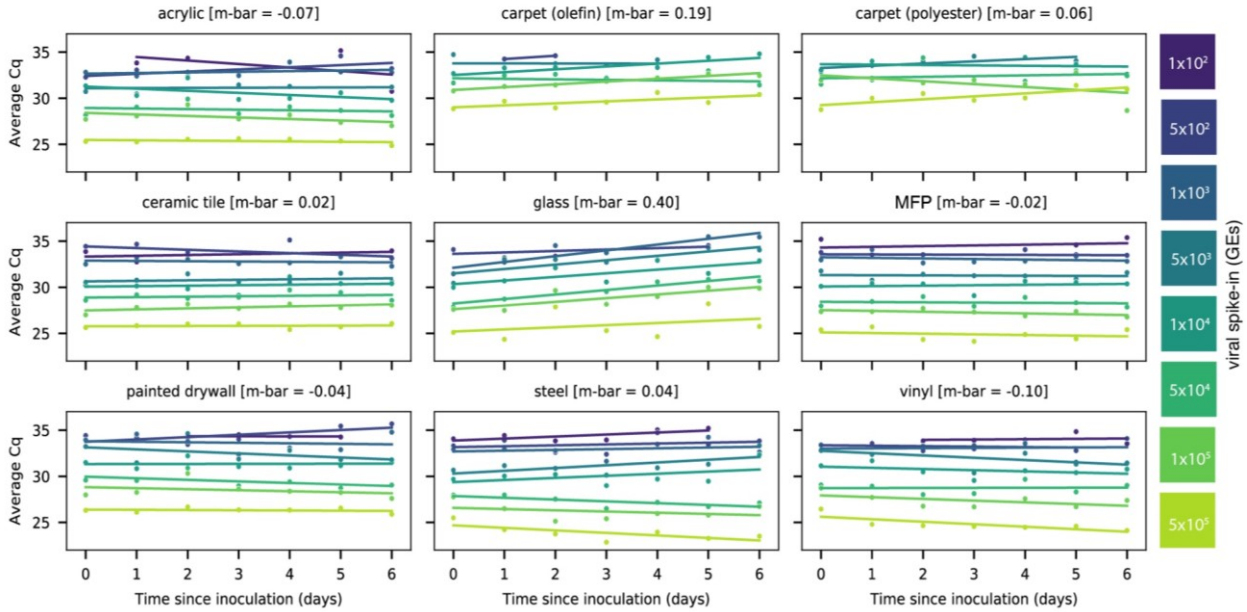

Figure 1: Scatterplots showing the average Cq of RT-qPCR viral gene calls for corresponding heat-inactivated viral spike-in over seven days. Viral spike-in concentrations reported as GE's from ddPCR. Linear regressions of average Cq on days since inoculation per spike-in were overlaid on the measured data. Average decay slope (m-bar) reported alongside each surface type.

A two-way repeated measure analysis of variance (ANOVA) on viral signal intensity (average *Cq*) revealed that surface type explains more observed variation in *Cq* than does time since inoculation at the highest concentration ($5x10^5$ GE's) (Fig. 2A). A Kruskal-Wallis *H* test confirmed that mean *Cq*'s differ significantly across surface types (H=61.63, p=1.78x10^-9)(Fig. 2B), but not across days since inoculation (H=0.89, p=0.99)(Fig. 2C). Pairwise Mann-Whitney *U* tests comparing ranked values of *Cq*'s from samples grouped by surface type highlight that both carpet materials (olefin and polyester) are significantly different, after correcting for multiple comparisons (FDR-Benjamini/Hochberg, alpha=0.005), from all other surfaces, but not from each other (Fig. 2B). Other pairwise, significant differences between materials are summarized in Supplementary Table S1. A clustermap of the *U* statistic from the pairwise comparisons effectively clusters samples by material properties, with rough surfaces clustering away from smooth ones (Fig. 2D).

Table S1: Statistically significant pairwise comparisons.

Surface Type	steel	vinyl	MFP	acrylic [infect.]	acrylic	glass	ceramic tile	painted drywall	carpet (olefin) [infect.]	carpet (olefin)	carpet (polyester)
steel	n.s.										
vinyl	n.s.	n.s.									
MFP	n.s.	n.s.	n.s.								
acrylic [live]	n.s.	n.s.	n.s.	n.s.							
acrylic	n.s.	n.s.	n.s.	n.s.	n.s.						
glass	n.s.	n.s.	n.s.	n.s.	n.s.	n.s.					
ceramic tile	**	n.s.	n.s.	n.s.	n.s.	n.s.	n.s.				
painted drywall	**	n.s.	**	**	**	n.s.	n.s.	n.s.			
carpet (olefin)	**	**	**	**	**	**	**	**	n.s.		
carpet (olefin)[infect]	**	**	**	**	**	n.s.	**	**	n.s.	n.s.	
carpet (polyester)	**	**	**	**	**	**	**	**	n.s.	n.s.	n.s.

*Table S1: Statistically significant differences from pairwise Mann-Whitney U tests between ranked values of average Cq from viral gene calls grouped by surface type after correction for multiple comparisons (FDR-Benjamin/Hochberg, alpha = 0.005)** (n.s.=Not Significant)*

Because RT-qPCR signal intensity for most surfaces was time invariant, time-collapsed linear regression models relating viral spike-in concentration (log2 spike-in) to average *Cq* act as standard curves for estimating viral load on different monitored surfaces from *Cq*. After segregating samples based on the qualitative material categories of smooth or rough, linear regressions aggregating all timepoints yielded one standard curve for smooth surfaces (m=-0.77, b=40.58, r=-0.93)(Fig. 2E) and another for rough surfaces (m=-0.47, b=39.40, r=-0.82)(Fig. 2F). The reduced slope of the latter curve stems from higher loss of spiked-in viral signal to the rough surface matrix.

Figure 2

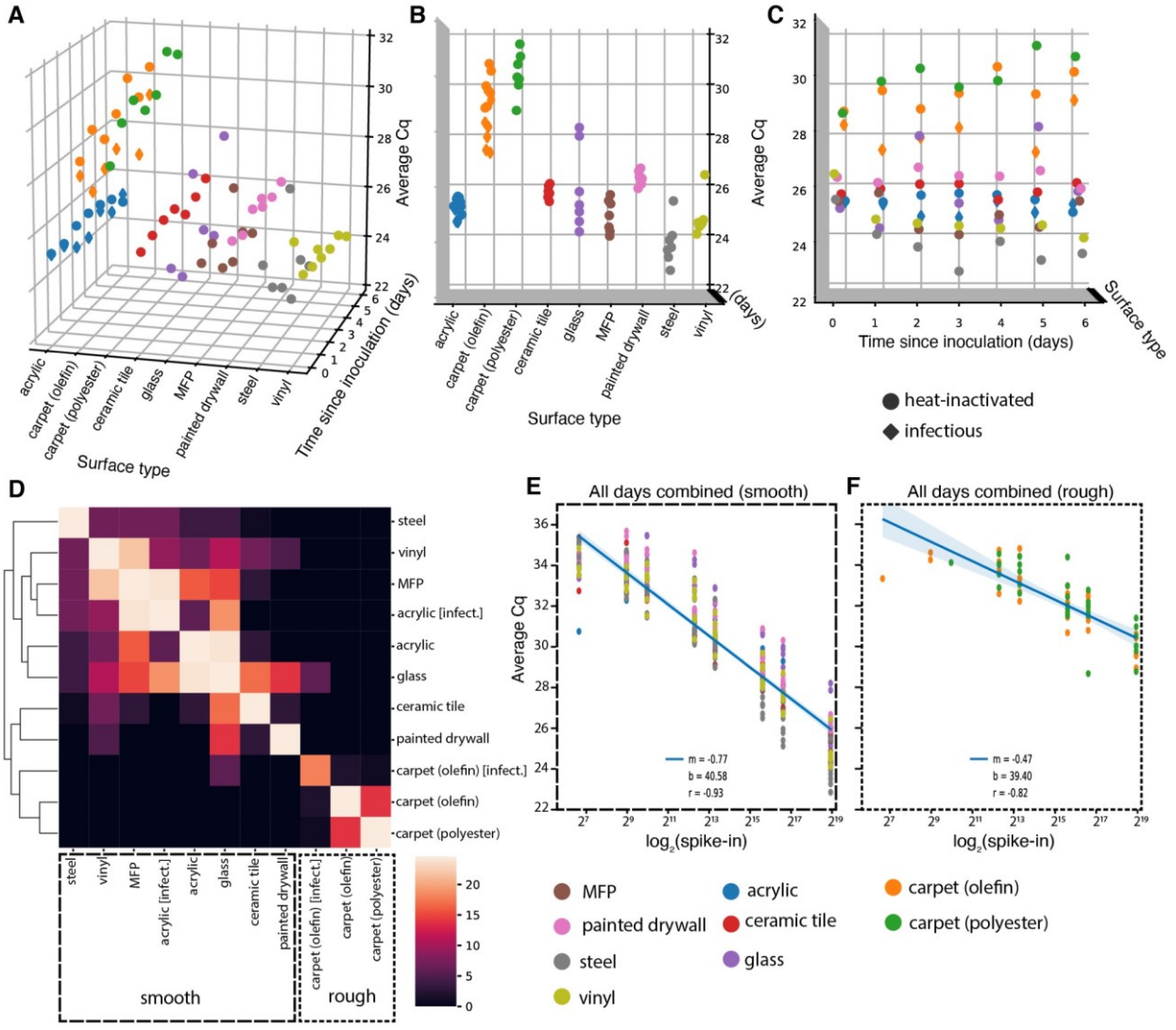

Figure 2: (A-C) 3D scatterplots showing distribution of average Cq of viral gene calls over seven days for nine different surfaces inoculated with 5x10^5 GEs (nine surfaces for heat-inactivated virus [circles], two (acrylic and olefin carpet) for infectious [diamonds]). The distribution of Cq's differs significantly across surface types (B), but not across days since inoculation (C). (D) Clustermap of the U statistic from pairwise Mann-Whitney U tests between surface types. (E-F) Standard curves relating surface viral load (spike-in) to average Cq across all time-points for smooth (E) and rough (F) surface types.

To ensure that viral signal stability was not a consequence of selection for resilient viral particles through heat inactivation, we repeated a subset of experiments using infectious virus in a BSL-3 laboratory using the B.1.351/Beta variant of SARS-CoV-2 originally identified in South Africa. Due to space limitations in the BSL-3 facility, the infectious virus experiment only included two surface types, acrylic and carpet (olefin), but used the same dilution series and sampling plan.

Results from infectious and heat-inactivated virus are concordant. Infectious virus samples cluster with respect to surface type rather than virion status (heat-inactivated or infectious) (Figure. 2D). When evaluating acrylic and carpet (olefin) samples alone, a Kruskal-Wallis *H* test shows significant differences in the means of Cq's across all groups when samples are grouped by surface type ($H = 16.25$, $p = 0.001007$) (Fig. S1A), but not when grouped by virion status ($H = 2.04$, $p = .153$) (Fig. S1B). Furthermore, linear regression on Cq from paired samples between the heat-inactivated and infectious virus experiments show nearly exact correlation ($m = 1.05$, $r = 0.97$) (Fig. S1C).

Figure S1

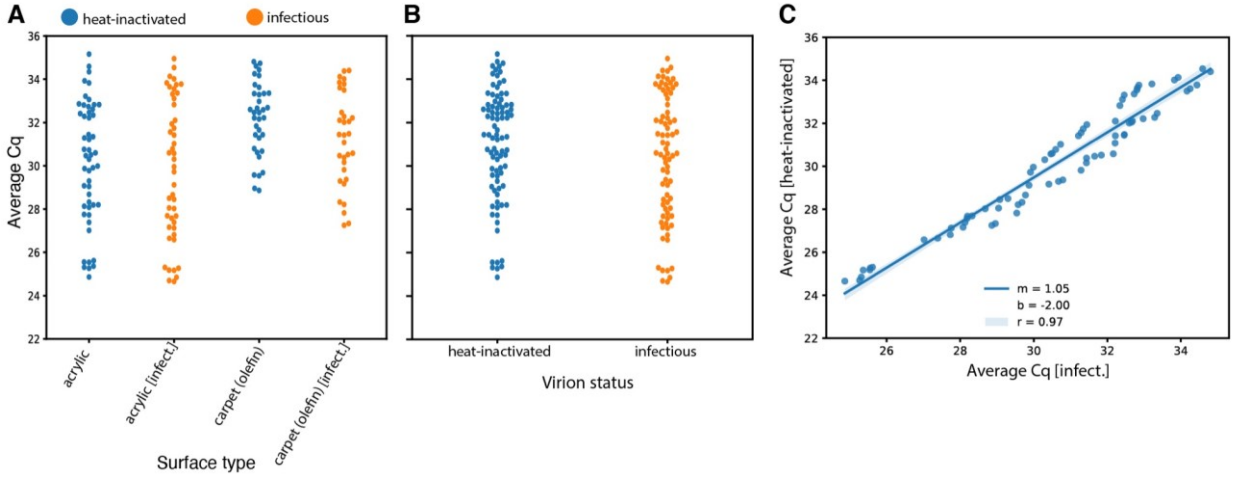

Figure S1. (A) Swarm-plot showing distribution of average Cq of viral gene calls for acrylic and carpet (olefin) surfaces for both heat-inactivated and infectious samples. (B) Swarm plot comparing distribution of average Cq of viral gene class for heat-inactived or infectious samples. (C) Linear regression on Cqs from paired samples between heat-inactivated and infectious samples.

Discussion

We show that detecting SARS-CoV-2 RNA on indoor surfaces in environments potentially exposed to COVID-19 infected individuals is effective across a variety of surfaces and a range of initial viral loads. Our swabbing and RT-qPCR methods have greater sensitivity from smooth surfaces (such as MFP - commonly found on desktops - or vinyl flooring) than rough surfaces (carpet). The stability of the viral signal across time limits the ability to estimate when the surface was inoculated, but demonstrates that signal can be detected a week post-exposure. To improve temporal resolution, surfaces swabbed for environmental monitoring should be cleaned with soap and water or disinfectant to remove viral signal [**14**], ensuring that subsequent SARS-CoV-2 detection results from separate exposures.

Although direct inoculation of surfaces with viral particles does not represent interaction with an infected individual in a real-world scenario, we do directly show that infectious and heat-inactivated SARS-CoV-2 particles have similar detectability and stability across surface types. These findings allow the use of heat-inactivated particles in testing and validating environmental

monitoring methods, and remove the burden of performing such experiments in BSL-3 laboratories.

Acknowledgements

We thank our partner schools and citizen scientists at 15 sites across 5 districts in San Diego county. This research was supported by NIH grant (K08AI130381) and a Career Award for Medical Scientists from the Burroughs Wellcome Fund to AFC, NIH grant (K01MH112436) to RFM, and the County of San Diego Health and Human Services Agency (Contract 563236). This work was performed with the support of the Genomics and Sequencing Core at the UC San Diego Center for AIDS Research (P30 AI036214), the VA San Diego Healthcare System, and the Veterans Medical Research Foundation. The following reagent was deposited by the Centers for Disease Control and Prevention and obtained through BEI Resources, NIAID, NIH: SARS-Related Coronavirus 2, Isolate USA-WA1/2020, NR-52281. The following reagent was obtained through BEI Resources, NIAID, NIH: SARS-Related Coronavirus 2, Isolate hCoV-19/South Africa/KRISP-K005325/2020, NR-54009, contributed by Alex Sigal and Tulio de Oliveira.

References

1. SASEA System – Safer At School Early Alert. Available at: https://saseasystem.org/. (Accessed: 1st July 2021)
2. Meyerowitz EA, Richterman A, Gandhi RT, Sax PE. 2021. *Transmission of SARS-CoV-2: A Review of Viral, Host, and Environmental Factors.* Ann Intern Med. NLM (Medline).
3. Parker CW, Singh N, Tighe S, Blachowicz A, Wood JM, Seuylemezian A, Vaishampayan P, Urbaniak C, Hendrickson R, Laaguiby P, Clark K, Clement BG, O'Hara NB, Couto-Rodriguez M, Bezdan D, Mason CE, Venkateswaran K. 2020. *End-to-End Protocol for the Detection of SARS-CoV-2 from Built Environments.* mSystems 5.
4. van Doremalen N, Bushmaker T, Morris DH, Holbrook MG, Gamble A, Williamson BN, Tamin A, Harcourt JL, Thornburg NJ, Gerber SI, Lloyd-Smith JO, de Wit E, Munster VJ. 2020. *Aerosol and Surface Stability of SARS-CoV-2 as Compared with SARS-CoV-1.* N Engl J Med 382:1564–1567.
5. Chin AWH, Chu JTS, Perera MRA, Hui KPY, Yen H-L, Chan MCW, Peiris M, Poon LLM. 2020. *Stability of SARS-CoV-2 in different environmental conditions.* The Lancet Microbe 1:e10.
6. Harbourt DE, Haddow AD, Piper AE, Bloomfield H, Kearney BJ, Fetterer D, Gibson K, Minogue T. 2020. *Modeling the stability of severe acute respiratory syndrome coronavirus 2 (SARS-CoV-2) on skin, currency, and clothing.* PLoS Negl Trop Dis 14:e0008831.
7. Renninger N, Nastasi N, Bope A, Cochran SJ, Haines SR, Balasubrahmaniam N, Stuart K, Bivins A, Bibby K, Hull NM, Dannemiller KC. 2021. *Indoor Dust as a Matrix for Surveillance of COVID-19*. mSystems 6.

8. Ye G, Lin H, Chen S, Wang S, Zeng Z, Wang W, Zhang S, Rebmann T, Li Y, Pan Z, Yang Z, Wang Y, Wang F, Qian Z, Wang X. 2020. *Environmental contamination of SARS-CoV-2 in healthcare premises.* J Infect 81:e1–e5.
9. Ben-Shmuel A, Brosh-Nissimov T, Glinert I, Bar-David E, Sittner A, Poni R, Cohen R, Achdout H, Tamir H, Yahalom-Ronen Y, Politi B, Melamed S, Vitner E, Cherry L, Israeli O, Beth-Din A, Paran N, Israely T, Yitzhaki S, Levy H, Weiss S. 2020. *Detection and infectivity potential of severe acute respiratory syndrome coronavirus 2 (SARS-CoV-2) environmental contamination in isolation units and quarantine facilities.* Clin Microbiol Infect 26:1658–1662.
10. Jiang FC, Jiang XL, Wang ZG, Meng ZH, Shao SF, Anderson BD, Ma MJ. 2020. *Detection of severe acute respiratory syndrome coronavirus 2 RNA on surfaces in quarantine rooms.* Emerg Infect Dis 26:2162–2164.
11. 1. Marotz C, Belda-Ferre P, Ali F, Das P, Huang S, Cantrell K, Jiang L, Martino C, Diner RE, Rahman G, McDonald D, Armstrong G, Kodera S, Donato S, Ecklu-Mensah G, Gottel N, Salas Garcia MC, Chiang LY, Salido RA, Shaffer JP, Bryant MK, Sanders K, Humphrey G, Ackermann G, Haiminen N, Beck KL, Kim HC, Carrieri AP, Parida L, Vázquez-Baeza Y, Torriani FJ, Knight R, Gilbert J, Sweeney DA, Allard SM. 2021. *SARS-CoV-2 detection status associates with bacterial community composition in patients and the hospital environment.* Microbiome 9:1–15.
12. Coronavirus (COVID-19) frequently asked questions | CDC. Available at: https://www.cdc.gov/coronavirus/2019-ncov/faq.html#Spread. (Accessed: 1st July 2021)
13. Science Brief: SARS-CoV-2 and Surface (Fomite) Transmission for Indoor Community Environments | CDC. Available at: https://www.cdc.gov/coronavirus/2019-ncov/more/science-and-research/surface-transmission.html. (Accessed: 1st July 2021)
14. Salido RA, Morgan SC, Rojas MI, Magallanes CG, Marotz C, DeHoff P, Belda-Ferre P, Aigner S, Kado DM, Yeo GW, Gilbert JA, Laurent L, Rohwer F, Knight R. 2020. *Handwashing and Detergent Treatment Greatly Reduce SARS-CoV-2 Viral Load on Halloween Candy Handled by COVID-19 Patients.* mSystems 5.